Toward hardware-driven simulation of underwater acoustic propagation and communication with Arctic ice, wind waves, and currents

Craig Hamm
Maritime Way Scientific Ltd.
Ottawa, Canada
craig.hamm@maritimeway.ca

Stephane Blouin
DRDC Atlantic Research Centre
Dartmouth, Canada
stephane.blouin@drdc-rddc.gc.ca

Martin Taillefer
Maritime Way Scientific Ltd.
Ottawa, Canada
mtaillefer@maritimeway.ca

***Abstract*—Maritime Way Scientific Ltd (MWS) in collaboration with the Defence Research and Development Canada, Atlantic Research Centre (DRDC-Atlantic) is developing a hardware-in-the-loop acoustic simulator for studying underwater acoustic propagation and the reliability of underwater communications signals. While the simulator can be used to model a wide variety of physical environments, most of the effort has been in adapting existing open source software (i.e. BELLHOP and VirTEX) to handle Arctic seas which may be either partially or fully covered with sea ice, using realistic keel morphology. As the project is still underway this paper presents the overall design, present capability, and some preliminary results. Areas for further improvement are also described.**

Keywords—simulation, hardware, communication, Arctic, sea ice, wind, currents

I. Introduction

The Arctic Ocean and its various shallow passages offer unique and challenging environments for underwater acoustic propagation and long-range acoustic communications. The underwater sound speed profile is predominately upward-refracting which increases the likelihood of interactions with the sea surface and wind-generated surface waves. The sea surface may also have a partial or a full ice cover of varying thickness and age. Arctic passages are relatively shallow, anywhere from 10 - 200 m, confining the sound within nearby reflective water column boundaries, strengthening multipath propagation. Both persistent and tidal currents flow through shallow channels, dynamically perturbing the sound speed profile. Cumulatively, these factors distort the integrity of propagated acoustic signals.

Arctic in situ testing is expensive due to the Arctic's extreme remoteness, difficulty of ship navigation in ice laden waters, and long periods of difficult weather. Therefore, the need for high-fidelity acoustic simulations becomes very attractive. A simulator can expose both the environmental and signal variables that most affect the acoustic propagation, and the reliability of underwater acoustic communication. Such a simulator can also assist with planning sensor placements prior to costly northern field deployments.

To the best of our knowledge, no research effort seems to deal with partial ice coverage, and no acoustic propagation simulator explicitly deals with water currents, with the former task being more complex than the latter. Recent acoustic channel simulators account for random variations in the channel [1, 2], though none accounted for sea ice. The work of Alexander, Duncan and Bose [3] and Alexander, Duncan, Bose, and Smith [4] examined acoustic propagation under ice canopies with 100% coverage. This single case is informative but restrictive as the Arctic region often experiences strong winds which generate stresses on the ice, leading to ice ridging or creating open water areas between sections of sea ice.

To address Arctic conditions, we are developing an underwater acoustic propagation and communications simulator which specifically deals with partial sea ice coverage, water currents, and wind waves. Further requirements of the system are to be able to capture real signals from any acoustic sensor and inject the captured signals into the simulated environment. In the case of communication sensors, *i.e.*, underwater acoustic modems, the simulator is to play the simulator-propagated signal back to the transmitting modem. This approach leverages the proprietary and protected manufacturer coding/decoding algorithms which are unavailable to us. These requirements necessitated and resulted in the design of a hardware-in-the-loop system.

II. Simulator System Overview

A. Hardware and Signal Flow

A diagrammatic overview of the simulator system is provided in Fig. 1. Components shown as shaded represent hardware, and data or software are shown as unshaded. Signal flow follows the directionality of the arrows. As the overall system still is under development, only the software components have been implemented and tested. The hardware integration phase is already initiated but still in its early stage.

The shaded components on the left-hand side of Fig. 1, labeled 'UW acoustic sensor' are defined first. The design allows for any reasonably-sized sonar sensor to be connected to the simulator and operated in air at low power to avoid damaging the sensor's transducer. Operational sensors such as underwater acoustic modems are depth rated and sealed by

This work has been supported by Defence Research and Development Canada (DRDC), DRDC-Atlantic Research Centre, under grant PWGSC W7707-145673."

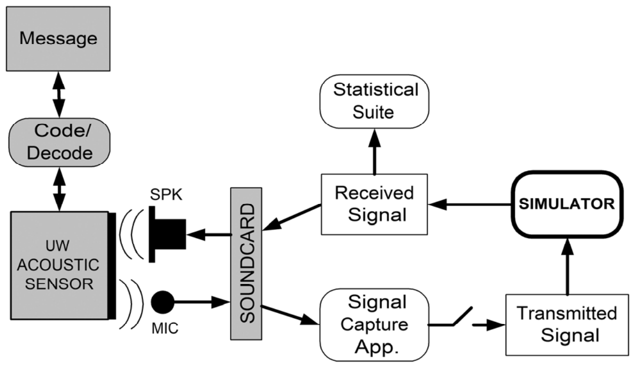

Fig. 1. Major components of the hardware in the loop underwater communications simulator.

manufacturers, thus making the acoustic-in-air test a viable choice as breaking the seal to access electrical interfaces within these units voids the depth ratings and also introduces other problems such as protection of circuit elements in the sensor and the sound card. Preliminary laboratory tests successfully demonstrated modem-to-modem communication in air. In the situation where the sensor is an underwater acoustic modem, messages may be sent to the modem via a serial interface, which could be scripted through a terminal emulator such as TeraTerm [5]. The sound generated, in air, by the sonar transducer is received by a Shure Beta 57A microphone (labeled 'MIC' in Fig. 1) which has a reasonably flat receive-response over its receive band. The host computer (not explicitly shown) is a high performance Dell Precision T7610 PC and contains all required software, described below. A high quality PC sound card (labeled 'SOUNDCARD' in Fig. 1) acts as the A/D and D/A for the system. A Xonar Essence STX audio card was chosen for this purpose. Normal audio system connectors are used for external connections.

When the underwater sensor is employed as the signal source, a dedicated 'Signal Capture Application' (Fig. 1), written in the C language, triggers the sound card output with a circular buffer and writes the captured signal to a standard .wav file format. When hardware is not employed, any .wav format file may be synthesized and passed to the simulator. The 'Simulator' software, described below, converts the 'Transmitted Signal' of Fig. 1 to the 'Received Signal' and saves it to a digital data file. Alternatively, when a simulated 'Received Signal' is required to excite the acoustic sensor, a speaker (label 'SPK' in Fig. 1) is driven by the sound card. The chosen speaker is the Wavecor TW030WA02, 30mm neodymium dome tweeter. With the on-axis transmit sensitivity and the sound card output capability, it is anticipated no further amplification will be required for the speaker.

B. Software

1) Overview

The key software components of the simulator are shown in Fig. 2. The main body of the simulator is a Matlab script fulfilling three main functions: i) a wrapper that manages all inputs for use by three open source models, BELLHOP [6] (propagation), VirTEX [7] (sea surface interaction) and WAFO [8] (sea surface definition) which are described below; ii) controls data flow to and from these models; and iii) directs outputs to the display and post processing statistical analysis

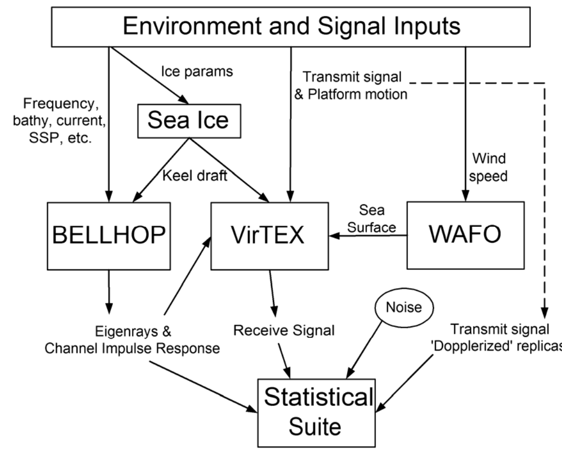

Fig. 2. Key software components of the simulator.

suite. The simulator may be run in BELLHOP-only mode, VirTEX-only mode, or a combined mode. These modes can facilitate different kinds of investigation, and each mode can be run either once (*i.e.*, one acoustic ping) or in a loop to gather statistics (*i.e.*, multiple acoustic pings, Monte Carlo simulation). During Monte Carlo runs the ping-to-ping variation arises from acoustic interaction with a time-varying sea surface (facilitated by VirTEX and WAFO), or through introducing different ice keel draft profiles at the sea surface. The ice keel draft model is described below.

2) Propagation Model

At its core, the simulator uses the Fortran model, BELLHOP, for determining the acoustic propagation. BELLHOP is a widely known open-source Gaussian beam ray-tracing propagation model in the underwater acoustic modelling community. Details on practical operation of BELLHOP may be found in user manuals [9,10] which also provide insight into the principles behind the technique used. Assuming water depths greater than ten-to-twenty acoustic wavelengths, ray-theory models are well-suited to a wide variety of frequencies, including those for underwater communication. As BELLHOP is a ray-based model, it is able to compute the time-of-flight for each eigenray (rays connecting only the source and receiver positions). These eigenrays terminate at the receiver position and define the underwater acoustic channel impulse-response, that is a set of n amplitudes at fixed corresponding times, $A_n(t_n)$. This channel impulse-response and the eigenray trajectories are both required to compute the received time series in post processing.

BELLHOP permits range-dependent environments to be defined and therefore surface altimetry can replace the, normally assumed, flat air-water interface. This is particularly useful for the inclusion of sea ice when the ice thickness and profile vary with range. In the presence of sea ice, the normal air-sea boundary is to be replaced by an acousto-elastic half-space defined by compressional and shear wave speeds (C_p, C_s), the material density (ρ), and compressional and shear attenuations (α_p , α_s). Typical values for those parameters are C_p = 3600m/s, C_s = 1800 m/s, ρ = 0.90 g/cm3, α_p = 0.07 dB/(m·kHz), and α_s = 0.41 dB/(m·kHz), based on averages found in Table 1 of [11].

Because partial (non-continuous) ice covers are implemented, BELLHOP was modified to differentiate between rays reflecting from the underside of ice on the top boundary versus reflection from those originating from the air-sea interface. The modification amounts to a short-term adaptation using a reflection coefficient of $R = -1+j0$ if the ray depth is less than 0.01 meters, indicating the air-sea boundary, otherwise the ray interacts with the sea ice lower boundary and the geoacoustic properties listed above are used. It is important to note that BELLHOP does not propagate energy through or within the upper half space. In future work, a higher-fidelity reflection model, such as that provided by using the BOUNCE program and used by Alexander, Duncan, Bose and Smith [4] may be considered.

3) Signal Convolution Model

To obtain the received signal, the convolution of the transmitted signal with the channel-impulse response is computed. However, given sea surface and source/receiver motions, the arrival structure amplitudes and delays require further corrections to account for these dynamic features. Whereas BELLHOP assumes a static environment and provides fixed arrival amplitudes, A_n, at fixed times, t_n, these amplitudes need to be generalized. The correct expression for the relationship between the transmitted signal, $s(t)$, and the received signal, $p(t)$, is described fully by Siderius and Porter [12] who provide the expression,

$$p(t) = \sum_{n=1}^{N} \mathrm{Re}[A_n(t)]s[t - \tau_n(t)] - \mathrm{Im}\,[A_n(t)]s^+[t - \tau_n(t)] \qquad (1)$$

where the $A_n(t)$ are time-dependent amplitudes (from the channel impulse-response), $\tau_n(t)$ is a time-dependent time delay, and s^+ is the Hilbert transform of $s(t)$. These time-dependent amplitudes and delays are computed by the open-source Matlab-based post-processor VirTEX (Virtual Time Series Experiment).

To compute the received signal, VirTEX performs the convolution in (1) after accounting for dynamic sea surface motion, source and receiver motion (defined by vertical and horizontal velocities), and an up-sampled version of the transmitted signal (*e.g.*, as output by a modem), with the eigenray trajectories and channel impulse-response. This is described in detail by Siderius and Porter [12]. Once computed, the received signal can be played through the soundcard, potentially to be decoded by a real acoustic sensor, be saved to a library of signals, or ingested by a suite of statistical/measurement routines.

To account for the inclusion of partial sea ice covers, VirTEX was also modified. Note that while the sea-surface is dynamic, the sea ice is stationary. VirTEX follows each eigenray and applies corrections due to a moving sea surface when the eigenray encounters the sea surface. When using partial ice covers, the key modification to VirTEX is to track instances when an eigenray encounters ice rather than the sea surface. Therefore, VirTEX was modified to read the BELLHOP altimetry file. If ice is encountered at the boundary, then no correction is applied.

4) Sea Surface Model

For generating spectrally accurate time-varying sea surfaces, VirTEX calls the open-source WAFO (Wave Analysis for Fatigue and Oceanography) Matlab Toolbox. The Pierson-Moskowitz wave spectrum [13] is employed, with sea surfaces being generated through a user specified wind speed.

5) Ice Keel Draft Model

The sea ice keel draft model is based on the work presented in Goff's paper [14] who sought to create a set of computational tools for estimating the stochastic properties of sea ice draft. Goff compared his method with statistically analyzed sea ice draft as measured using by upward looking sonar under a 10 x 10 km square section of Arctic ice, with a good measure of success. The method provides a recipe for computing ice keels that very closely match five parameters used to classify real terrains, namely the mean thickness (t_0), RMS thickness (H), normalized skewness (μ_3^n), characteristic length scale (λ_θ), and fractal dimension (D). A sample ice keel section of 2000 meter in length is shown in Fig. 2 for inputs, H = 3.84 m, t_0 = 4.52 m, λ_θ = 63.8 m, D = 1.26, μ_3^n = 1.27, corresponding to Fig. 6 from Goff [14]. Randomly distributed partial ice covers are generated by first generating a full-range ice cover and then replacing random length sections by zeros, at random starting locations. This is done iteratively, with the covered fraction being measured and compared to the desired fraction at each step. If the desired fraction is exceeded the process is repeated until the desired fraction is attained.

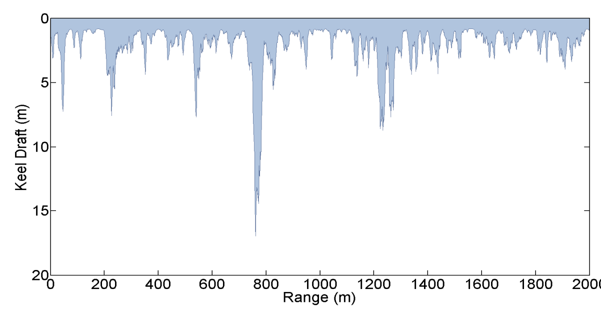

Fig. 3. Sample output from the ice keel draft model.

6) Water Currents

There are several ways to express the speed of sound in moving media. One technique, shown in Thompson [15], was to derive the equivalent Snell's Law. Ray tracing may be performed by integrating the following equations with respect to x (equivalently, range):

$$\frac{dZ}{dx} = \tan\alpha \qquad (2)$$

where Z is the depth in the water, α is the ray launch angle (from the horizontal, positive clockwise) and with the inclusion of current it can be shown that,

$$\frac{d\alpha}{dx} = -\frac{c_z + U_z \sec\alpha}{c + U \sec\alpha} \qquad (3)$$

for small Mach numbers ($M = U/c$), U is the speed of water current (a function of depth), c is the speed of sound (a function of depth), and c_z and U_z are shorthand variants for vertical derivatives (gradients) dc/dz and dU/dz, respectively.

For natural flows, the Mach number is of order $M \ll 1$, and so the $U \sec \alpha$ term in the denominator is quite small and serves mainly as a perturbation to the sound speed, and hence time-of-flight (about 0.5 ms/km per m/s of current). Sanford [16], provides insights with respect to the effects of current shear. The presence of the current gradient, U_z, in the numerator of equation (3) may be comparable to, or greater than, the sound speed gradient, c_z. This may be significant, as even in an isovelocity environment (*i.e.*, c_z=0) any remaining current gradients will refract sound and determine eigenrays that might otherwise note have been expected. Hence, the channel impulse response may be, likewise, affected.

For moderate ray launch angles ($\alpha \leq 30^o$), equation (3) may be simplified to a 'summed' sound-speed-plus-current approach,

$$\frac{d\alpha}{dx} = -\frac{(c+U)_z}{(c+U)} \quad (4)$$

In the numerator of equation (4), the sound speed (at depth Z) and the current speed (at depth Z) are summed, and then the vertical derivative is calculated. In the denominator, only the sum is taken. The implications of this are that for moderate angles the current may be added to the sound speed profile outside of the propagation model and then presented to the model as new sound speed profile: $c_{\text{new}}(z) = c_{\text{actual}}(z) + U(z)$, without requiring changes to the propagation model code. As the water current is signed (or has a directionality), the introduction of water current leads to a loss of acoustic reciprocity in the channel. That is, the transmission loss calculated between points A and B, is no longer the same as from B to A. Thus, in the presence of significant current (and its gradient), the simulator should be able to reverse the environmental inputs to calculate this B to A propagation. This capability has been implemented as a single input switch to reverse the entire A to B scenario.

Salomans [17] discusses moving-medium effects in the atmosphere. For Mach numbers similar to our expected values, he demonstrates that the simple addition of the wind speed in the in-line direction was an accurate approximation. His tests included comparisons between a ray model and a Fast Field Program (FFP) method and found that in the frequency range of the ray theory, the results matched. The conclusion is that the method using equation (4) is sufficient for use in the simulator as long as the current profile is sampled such that all significant current gradients are adequately resolved. Not capturing these current gradients will result in poor prediction performance. Experimental validation of this assertion, using stratified tidal flows, is identified as part of future work.

7) Signal Generation

By default the simulator operates on digital signal data saved as a .wav formatted audio file. With little effort the simulator can be changed to accept other formats. These data may originate from any source such as signal generation hardware, sonar generated, or from a built-in simulator signal suite. Signals are generated by this suite are via built-in Matlab functions, or custom functions. Signals presently available in the simulator are multiple frequency shift keying (MFSK), binary phase shift keying (BPSK) using the method of Borowski [18], Linear and Hyperbolic Frequency Modulated (LFM, HFM), and continuous wave (CW). In the case of modulated coded signals, the corresponding demodulator is available.

III. Preliminary Results

This section presents the effects of partial ice cover and wind on acoustic propagation and communication performance in a shallow channel, as calculated by the simulator described above.

A. Effects of Partial Ice Covers on Propagation Loss

Fig. 4 shows the full-field coherent propagation loss as computed by BELLHOP. The environment is 200 m depth, and 15 km in range. The bottom is flat (muddy sand) and the surface boundary is a partial ice cover with 60% coverage over the entire range, *i.e.* 60% of the sea surface is covered in sea ice of varying thickness, and 40% of the sea surface is exposed to air. The ice, barely visible in Fig. 4, was generated using the method described, above. The source is of a sufficiently high frequency such that the BELLHOP model is readily applicable, and whose wavelength is much smaller than any single physical feature in the environment. The source is shown, located at zero range and a depth of 20 m. An upward refracting sound speed profile, common in the Arctic, is applied to all ranges, with the sound speed being 1500 m/s at the surface and increases linearly to 1520 m/s at the sea bed depth of 200 m. This simple sound speed profile is useful for the purposes of testing. This sound speed profile is used throughout this section. The shading indicates relative intensity of the sound, with light to darker shading indicating higher to lower acoustic intensities, respectively.

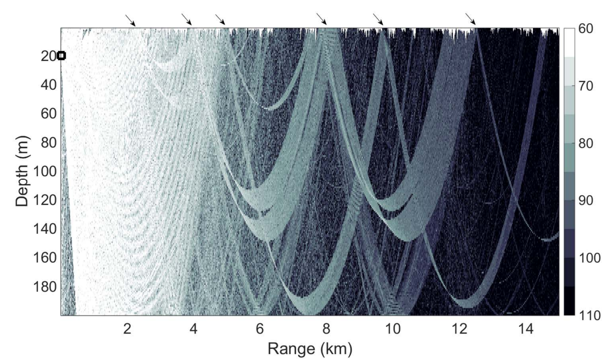

Fig. 4. Sample full-field propagation loss for an ice canopy with 60% partial coverage.

A signature feature of the sound field under a partial ice cover is that energy propagates in spatial *ribbons*, which are visible in Fig. 4 as refracted energy of a lighter shade than the background. These ribbons occur as a result of stronger reflection from the sea surface air-water interface as compared to reflection and scattering from the underside of the solid ice canopy. In this sample, reflections from short sections of air-water interface, at approximately 2.5, 4 and 5 km, create this structure in the water that influences the field at much farther ranges. In this type of environment the spatial structure of the sound field at longer ranges is highly dependent upon the initial condition, the location of the transmitter with respect to the surface ice features. Likewise, for fixed transmitter and receiver locations, if the ice cover drifts under the influence of surface currents, or winds, the receiver will experience wide variations in signal strength over time.

B. Eigenray variability

Fig. 5 shows two eigenray plots for a similar environment as in Fig 4, but to range of 5 km, and for two different partial ice covers, each of 50%. The source is at 20 m depth, and the receiver may represent a bottom moored sensor, floating 10 m above the seafloor at 190 m depth. Each plot was extracted from a set of runs in a Monte Carlo simulation which was used to assess bit error rate (BER), discussed below. Immediately one observes the vast difference in the number of eigenrays between the two realizations. Over a single series of 30 realizations it is not uncommon to observe extremes showing as few as 10 eigenrays to as high as 40 eigenrays. Second, one observes that many eigenrays make contact with the ice canopy. Many of these rays might not have been found as eigenrays had it not been for luck in intersecting a random perturbation from the surface altimetry enabling the source to receiver connection. However, it also appears as though the ice canopy introduces a lot of steep angle propagating rays. These rays will arrive much later and likely with higher attenuation due to the accumulation of losses encountered at the boundaries.

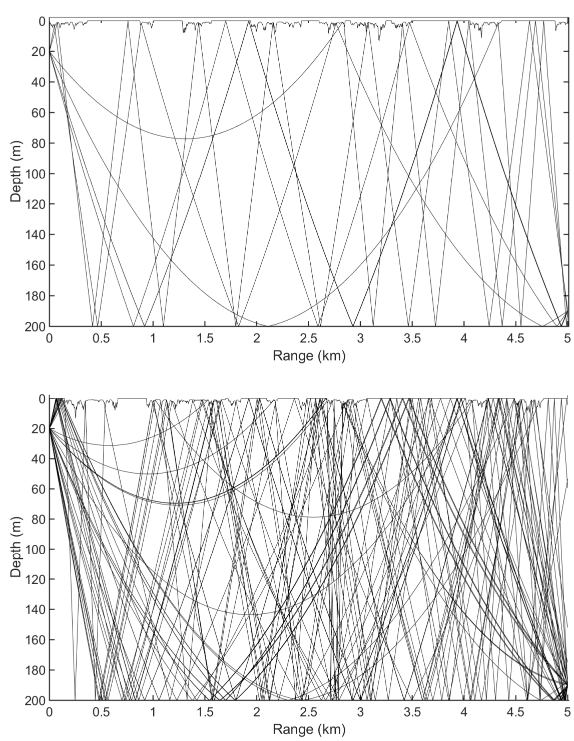

Fig. 5. Eigenray plots for two different instances of 50% partial ice coverage. Upper plot shows a low number of eigenrays (7). Lower plot shows very many eigenrays (>30).

C. Effects on communication

The results of this section are to be considered preliminary. It is of interest to understand how partial ice covers affect the reliability of acoustic communication between a source and a receiver. The environment and source-receiver geometry are the same as described in III-B, however the partial ice coverages were: 0% (no ice, full exposure to wind), 20%, 50%, 80%, and 100% coverage (no exposure to wind). For each of these ice coverage percentages, three wind speeds were used: 0 (no wind), 5 m/s, and 10 m/s. The sea surface spectrum, as generated by WAFO, used a Pierson-Moskowitz spectrum [13]. The signals used were random sequences of 0 and 1, binary phase shift key (BPSK) encoded, and transmitted on a carrier. The signals were 3 seconds duration, and two low bit rates were used: 25 and 50 bits per second (bps), respectively. For each combination of inputs 30 realizations were generated from which the mean BER and the standard deviation were computed. The BER rate is calculated immediately upon demodulation by comparing the decoded received binary sequence of 0's and 1's to the known transmitted sequence. The demodulator (after Borowski [18]) is robust, using both a training byte prior to the binary message, and a FM-chirp signal, to synchronize the receive pulse. All calculations were done in the absence of any random noise. Therefore, this example represents a high signal-to-noise ratio (SNR) case.

The preliminary results are shown in Fig 6. The BER is displayed along the vertical axis, and the percentage of ice cover is shown along the horizontal axis. Overall, the BER appear high, with nearly all signals exhibiting average BER values of 0.1 (10% incorrect) or worse regardless of wind speed or ice cover. As the wind speed increases from zero to 10 m/s the BER increases, as one expects, from increased sea surface wave motion. In the high wind speed case (10m/s) the BER decreases as the percentage of ice cover increases to 100%. This is expected as the sea ice in our present model is motionless and therefore increased ice cover protects the propagating signal from the effects of the sea surface motion. Finally, the data converge when the ice cover is 100% where the wind has no effect on any signal.

The effect of changing the bit rate from 25 to 50 bps made no significant difference. The dip in BER at 50% for zero wind speed ice cover stands out as slightly counter intuitive. This datum was checked by running another Monte Carlo set, and the result was effectively the same.

The variability in the mean BER is discussed next. Not shown in Fig. 6 are the ±1 standard deviation bars. The standard deviations all fell within the range 0.11 to 0.24 (except, zero for wind speed 0 m/s, and 0% ice cover, which is a single run). Typical standard deviations were near the value 0.15, even when the BER was less than 0.15, such that many single realizations were observed with BER = 0.0 (perfect decoding). Conversely, it is common to see the BER > 0.3 in the same set of values, as is shown in Fig. 7 (for zero wind speed) for a different ice canopy. These large variations in BER appear to be in line with the previous assertion that with any ice cover, the acoustic field at the receiver is highly susceptible to the particular ice canopy.

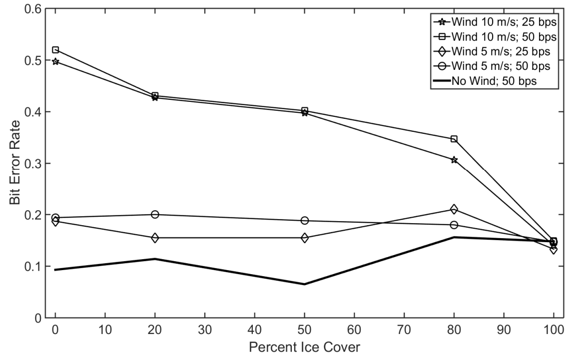

Fig. 6. Bit error rate (BER) plotted against percentage of ice cover for three wind speeds.

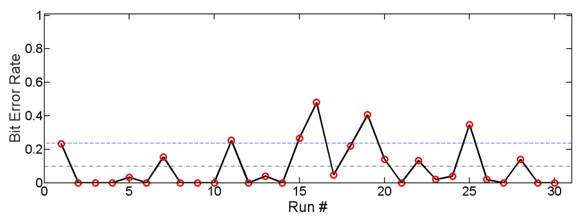

Fig. 7. Example of BER variability across different realizations within a Monte Carlo run (wind speed 0 m/s, ice cover 20%).

IV. Future Work

As the project progresses, both lab studies and field studies will be conducted. As part of refining and extending the study presented here, we should perform larger Monte Carlo runs for improved statistics, find a selection criteria for determining improved bit rate for test, and also examine BER variability under partial ice covers due to small changes in transmitter and receiver position with respect to the ice cover position. Coloured noise will be added to the code suite. As hardware is obtained, the hardware-in-the-loop portion will be assembled and tested with real sonars mounted to the test bench. Preliminary field work has occurred but the conditions were problematic and there is a desire to repeat these experiments in the presence of tidal currents that we wish to report on.

Acknowledgment

The authors thank Dr. Sean Pecknold, Dr. Diana McCammon, Dr. Gary Brooke, and Dr. John Goff for valuable comments and assistance during the course of the development and preparation of the paper.

References

[1] Q. Parastoo, M. Stojanovic, “Statistical characterization and computationally efficient modeling of a class of underwater acoustic communication channels,” IEEE Journal of Ocenanic Engineering, 38, 4, p. 701-717, 2013.

[2] H.S. Dol, M. E.G.D. Colin, M.A. Ainslie, P.A. van Waltree, “Simulation of an underwater acoustic communication channel characterized by wind-generated surface waves and bubbles,” IEEE Journal of Ocenanic Engineering, 38, 4, p. 642-654, 2013.

[3] P. Alexander, A. Duncan, N. Bose, Modelling sound propagation under ice using the Ocean Acoustics Library's Acoustic Toolbox, in McMinn, Terrance (ed.), Acoustics 2012 Fremantle: Acoustics, Development and the Environment, Conference of the Australian Acoustical Society, Nov 21-23 2012, Fremantle, Western Australia.

[4] P. Alexander, A. Duncan, N. Bose, D. Smith, “Modelling acoustic transmission loss due to sea ice cover,” Acoustics Australia, 41, 1, April 2013.

[5] Tera Term homepage: http://ttssh2.osdn.jp/index.html.en (last accessed 10 Aug 2015).

[6] M. B. Porter, Acoustic Toolbox distributed under the GNU Public License, http://oalib.hlsresearch.com/Modes/AcousticsToolbox/ (last accessed 10 Aug 2015).

[7] J.C. Peterson, John C., M.B. Porter, Virtual Timeseries Experiment (VirTEX) - Quick Start, 8 July, 2011. (http://oalib.hlsresearch.com/Rays/index.html, last accessed 10 Aug 2015).

[8] “WAFO— A Matlab toolbox for analysis of random waves and loads, tutorial for WAFO v2.5,” Lund Univ., Lund, Sweden, 2011 [Online]. Available: http://www.maths.lth.se/matstat/wafo (last accessed 5 Aug 2015).

[9] M.B. Porter, The BELLHOP manual and user’s guide: PRELIMINARY DRAFT, Heat, Light, and Sound Research, Inc., La Jolla, CA, USA, January 31, 2011.

[10] O.C. Rodriguez, General description of the BELLHOP ray tracing program (June 2008 release), Physics Department, Signal Processing Laboratory, Faculdade de Ciencias e Tecnologia Universidade do Algarve, Version 1.0, 2008.

[11] D.F. McCammon, S.T. McDaniel, The influence of the physical properties of ice on reflectivity, J. Acoust. Soc. Am., 77 (2), February 1985, p. 499-507.

[12] M. Siderius, M.B. Porter, “Modeling broadband ocean acoustic transmissions with time-varying sea surfaces,” J. Acoust. Soc. Am. 124 (1), p. 137-50, July 2008.

[13] W.J. Pierson, L.A. Moskowitz, “Proposed spectral form for fully developed wind seas based on the similarity theory of S. A. Kitaigorodskii,” Journal of Geophysical Research, Vol. 69, p.5181-5190, 1964.

[14] J.A. Goff., “Quantitative analysis of sea ice draft 1. Methods for stochastic modeling, Journal of Geophysical Research,” Vol. 100, No. C4, p. 6993-7004, 1995.

[15] R.J. Thompson, “Ray theory for an inhomogeneous moving medium,” J. Acoust. Soc. Am. 51, (5) (Part 2), 1972.

[16] T.B. Sanford, “Observations of strong current shears in the deep ocean and some implications on sound rays,” J. Acoust. Soc. Am., 56 (4), October 1974.

[17] E.M. Salomans, Computational Atmospheric Acoustics, Kluwer Academic Publishers, Norwell, MA, USA, 2001 (see section 4.6).

[18] B.S. Borowski, Application of channel estimation to underwateracoustic communicaton, Ph.D. dissertation, Stevens Institute of Technology,Castle Point on Hudson, Hoboken NJ, 2010.